Transactions of the Korean Nuclear Society Virtual Autumn Meeting
October 21-22, 2021

Aerosol Removal by Dry Tube Bundle in Steam Generator

Byeonghee Lee* and Kwang Soon Ha
Korea Atomic Energy Research Institute, Daedeokdaero 989-111, Yuseong, Daejeon, Korea 34057

*Corresponding author: leebh@kaeri.re.kr

1. Introduction

The steam generator (SG) is the primary route of radioactive materials before releasing to environment when a steam generator tube ruptures (SGTR). Especially, when a severe accident with the SGTR occurs, a large amount of the fission products releases to the environment bypassing the containment, threatening the public health goal. The recent legislation about severe accidents in Korea set the quantitative goal of fission product release to the environment, for protecting the public from excessive radiological exposures. The SGTR induced by a severe accident is therefore important although the occurrence probability is very low.

Therefore, the aerosol removal in SG is important when estimating the radiological consequences by the SGTR, because a lot of fission product is expected to be removed in SG due to the complex geometry and the large surface area in it. The aerosol removal depends a lot on the flooding condition in SG, however, the typical scenario of SGTR occurs when the SG is in dry condition [1]. Several mechanisms such as inertial impaction, turbulent deposition, or gravitational settling work together for the aerosol removal in SG.

In this article, the aerosol removal tests were conducted for the dry tube bundle using the AEOLUS facility built in KAERI. And the simplified analyses for the expected aerosol removal mechanisms were also performed to see the physics of aerosol removal in SG.

2. Experimental Facility

Figure 1 shows the schematic of the AEOLUS (Aerosol Experiments on LWR under SGTR) facility used for the experiment. The AEOLUS is composed of an aerosol generation system, a test vessel including the tube bundle, and multiple aerosol sampling systems. In this experiment, the 1m-long tube bundle composed of 270 individual tubes are installed in the vessel.

As the aerosol material, monodispersed SiO_2 particles with mass mean diameter (MMD) of 0.7 μm were used. The SiO_2 particles were dispersed in ethanol with 10% wt., and the fluid were ejected into the mixing chamber with hot carrier gas at the same time. Then the ethanol evaporates in the hot chamber and the SiO_2 particles are disperse in the carrier gas as aerosols. Then the aerosol laden gas was supplied into the vessel through the center tube. The center tube had circumferential openings to simulate the guillotine break of the SG tube, and the gas was ejected through the break perpendicularly to the surrounding tube bundle. The aerosols in the gas were then removed by the tube bundle, and flowed out to the outlet pipe connected to the vessel top.

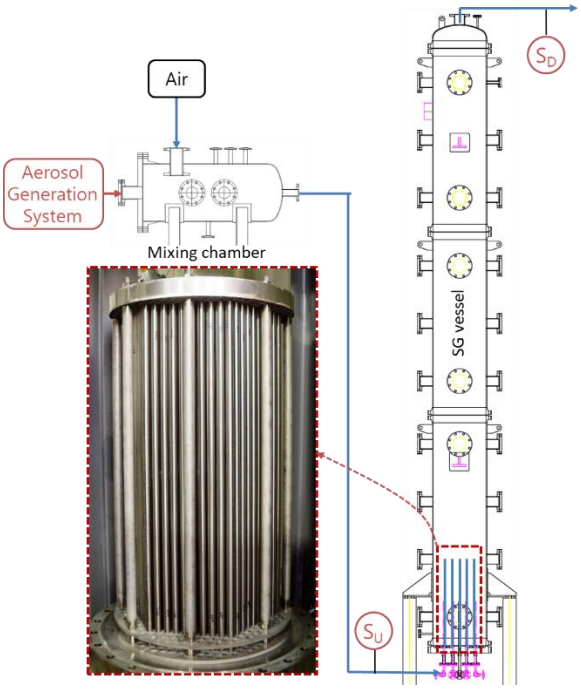

Fig. 1 Schematic of Experimental Facility (AEOLUS)

The aerosol sampling systems were installed at the inlet and at the outlet of the facility to measure the aerosol concentration at the positions. The aerosol laden gas was sampled with the sampling nozzle under an isokinetic condition, and flowed through the glass fiber filter to collect the aerosol particles. The aerosol concentration was then calculated from the sampled gas volume and the collected aerosol mass on the filter. At the same time, the electrical low pressure impactor (ELPI, DEKATI^{TM}) were used to check the real-time aerosol concentration and size distribution, however, was only used for a monitoring purpose.

Table 2 shows the thermal-hydraulic condition of the test. The carrier gas was air instead of steam to neglect the aerosol removal by the condensation, resulting in more conservative results. The actual primary pressure during SGTR is higher than 150 bar abs, however, is not practical for the test condition. Instead, the primary pressure in the test were set sufficiently high such that the jet from the break was in choked condition. And the inlet temperature was set higher than the saturation temperature at that pressure. The downstream pressure was about 2.3 bar, which is slightly increased for ease of the sampling. The mass flow rate of the air were about 0.17 kg/s. The carrier gas were heated by the steam heater and by the wall of the vessel and the pipes which are electrically heated. The sampling tubes were also electrically heated to minimize the thermophoresis.

Table 1 Experimental Condition

Variable	Value
Working fluid	Air
Upstream pressure (bar)	6.9
Downstream pressure (bar)	2.3
Inlet gas temperature (°C)	~160
Mass flow rate (kg/s)	0.17
Aerosol Particle	SiO_2 (MMD 0.7μm)

3. Experimental Results

Table 2 shows the estimated decontamination factor of the test. The aerosol sampling was conducted three times with 1800 s per each. The decontamination factor is calculated by comparing the aerosol concentration of the inlet and outlet as

$$DF = \frac{C_{in}}{C_{out}}$$

where C is the aerosol concentration (mg/m^3). The average DF of all three sampling were 4.0.

After finishing the filter sampling tests, the SG vessel were opened and the individual tubes were disassembled from the tube bundle. The aerosol deposited on the tube was then collected for each tube along the six major directions (N, NE, SE, S, SW, NW), and the mass of collected aerosol was measured for each tube.

Figure 2 shows aerosol deposition pattern on the tube bundle The picture shows white aerosol deposited on the stainless steel tube bundle, which generally deposited upward due to the bulk fluid direction. Near the jet exit of the center tube, the aerosol seems washed out by high kinetic energy of the jet, and re-attached on the center tube after rebound on the adjacent tubes.

The figure also shows the measured aerosol mass on the tube with respect to the distance from the center tube where the jet ejected. The aerosol mass deposited on tube initially increases to the 2nd tube, and then decrease with distance. The reason of initial increase is that the aerosols deposited on the 1st tube are washed out by the high speed jet from the break.

The aerosol mass was measured for only 54 tubes, 9 tubes for the 6 directions, then extrapolated for entire tubes, by assuming that the n-th tubes from the center have the same amount of aerosol deposited on them. By the extrapolation, the total amount collected by the tube was about 117g.

Table 2 Estimated Decontamination Factor

Variable	Value
Sampling	3 times
Sampling duration	1800 s
Average DF	4.0
Collected aerosol from the tubes (extrapolated)	117 g

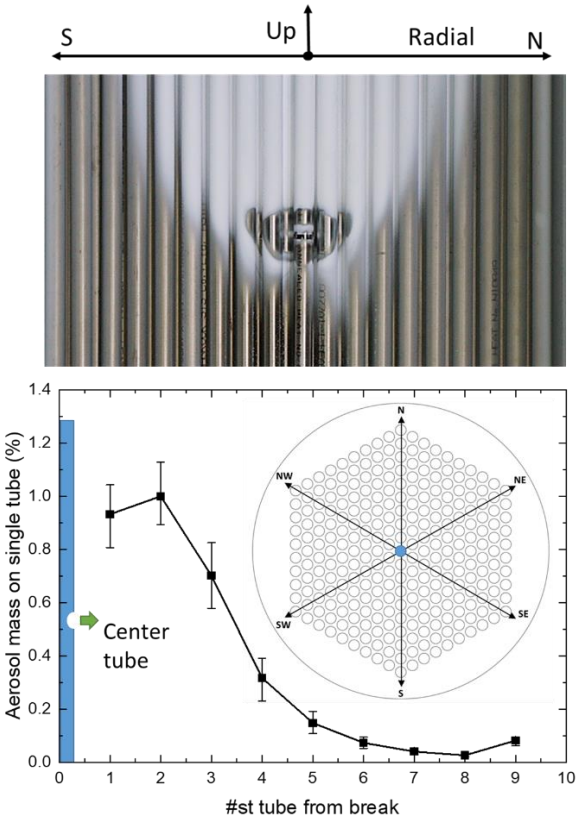

Fig. 2 Aerosol deposition on tube bundle (top) and deposited mass on single tube versus distance

4. Analysis of Aerosol Removal

Table 3 shows the various mechanisms of aerosol removal applicable for the AEOLUS dry bundle test. The mechanisms are independent from each other, and each mechanism can be estimated roughly by relative nondimentional parameters. Among the mechanisms, the gravitational settling and the Brownian diffusion are negligibly small for our experimental condition. The thermophoresis was excluded from the list because the vessel and the tube bundle are in isothermal condition. Therefore, the aerosol collection by the turbulent deposition, the inertial impaction, and the interception were considered in the calculation.

Figure 3 shows the 1-D modeling of the aerosol removal by tube bundle by a filter approximation. When a monodispersed particle laden flow passes through the cylindrical fibers, the overall collection efficiency by the fibers can be expressed by [2]

$$\eta_{TB} = 1 - exp\left(-\int_0^L \frac{4\eta_{ST}}{\pi D}\frac{\alpha}{1-\alpha}dl\right)$$
$$\approx 1 - exp\left(-\sum_{i=0}^{N}\frac{4\eta_{ST}}{\pi}\frac{\alpha}{1-\alpha}\frac{\Delta L}{D}\right)$$

where η_{TB} and η_{ST} are the collection efficiency of the tube bundle and the single tube, respectively, and α is the volume fraction of tubes.

Table 3 Estimated Decontamination Factor

Mechanism	Parameter	Approx. Value	
		Near field	Far field
Turbulent deposition	$Sc_T \cdot Re_g^{0.5}$	~10^0	~10^{-2}
Inertial impaction	Stk	~10^{-2}	~10^{-4}
Interception	d_p/D	~10^{-5}	
Gravitational settling	$\frac{v_{TS}}{U} = \frac{\rho d_p^2 C_c g}{18\mu U}$	<10^{-7}	
Brownian diffusion	$2Pe^{-2/3}$	<10^{-5}	

$Sc_T = \frac{\mu}{\rho D_T}$; Turbulent Schmidt number

$Re_g = \frac{\rho UD}{\mu}$; Gas Reynolds number

$Stk = \frac{\rho_p d_p^2 U}{18\mu D}$; Particle Stokes number

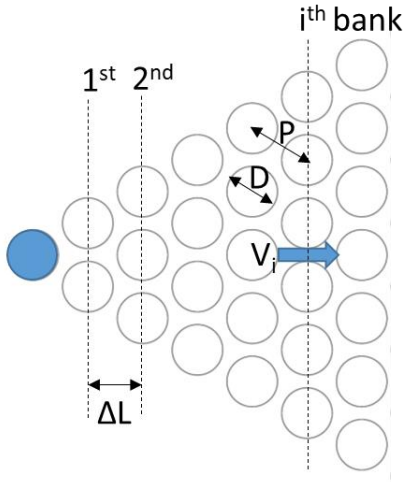

Fig. 3 1-D calculation of aerosol collection

The collection efficiency of single tube can be expressed for each collection mechanism. The collection efficiency by turbulent deposition is fitted from the exiting experimental data by [3]

$$\eta_{TB\_TD} = 0.438 + 0.0713\ln(Stk_e)$$

where Stk_e is the effective Stokes number considering the effect of particle Reynolds number as

$$Stk_e = Stk\Psi(Re_p)$$

where $\Psi(Re_p) = \frac{3\left[0.158^{0.5} Re_p^{\frac{1}{3}} - \mathrm{atan}\left(0.158^{0.5} Re_p^{\frac{1}{3}}\right)\right]}{0.158^{0.5} Re_p}$.

The collection efficiency of single tube by impaction and interception was derived as [2]

$$\eta_{TB_{Imp\&Int}} = \frac{1-\alpha}{Ku}\left(\frac{d_p}{D}\right)^2 + \frac{2(1-\alpha)\sqrt{\alpha}}{Ku} Stk_e \left(\frac{d_p}{D}\right) + \frac{(1-\alpha)\alpha}{Ku} Stk_e$$

where Ku is the Kuwabara factor defined by

$$Ku = \alpha - \alpha^2/4 - 3/4 - (1/2)ln\alpha$$

All the above equations, the flow velocity is the critical parameter for calculation. The 1-D flow velocity striking i^{th} bank tubes is approximated as

$$V_i = \frac{1}{2^i} V_o$$

where V_0 is the velocity at the break exit.

Table 4 shows the geometric parameters used for the calculation. The tube size, the pitch between tubes were from the actual tube geometry, and the volume fraction was calculated from the diameter and the pitch. With the geometrical information of the tube bundle and the thermal hydraulic information from the experimental condition, the collection efficiencies were calculated for i^{th} bank bundle tubes, and then the total collection efficiency by the bundle was estimated from them.

After the collection efficiency was calculated with the 1-D filter approximation, the collection efficiency of the experiment was calculated from the extrapolated sum of aerosol on i^{th} bank tubes divided by the total supplied aerosol mass during the experiment. The total supplied aerosol mass was calculated from the inlet aerosol concentration multiplied by the supplied gas volume during the aerosol generation.

Figure 4 shows the collection efficiency of the i^{th} bank tubes estimated from the experiment and the calculation. For the 1st and 2nd bank tubes, the collection efficiency from the experiment were significantly smaller than those from calculation, because of the washing out of aerosol near the jet exit. The high speed jet from the break washes out the deposited aerosol, and at the same time, prevents the aerosol deposition near the jet. The resuspended aerosol can move to the next bank tubes, and deposited there. From the 6^{th} bank tubes, the aerosol deposition was calculated to be zero, whereas the experiment still shows small portion of deposition. On the 9^{th} bank tubes, the aerosol deposition increases a little comparing to the 8^{th} bank tubes, because of the flow recirculation between the outmost tubes and the vessel wall promotes the aerosol deposition.

Table 4 Parameters used for calcuation

Variable	Value
Diameter of tube (mm)	19.0
Tube pitch (mm)	25.4
Pitch to diameter	1.33
Volume fraction of tubes	0.51

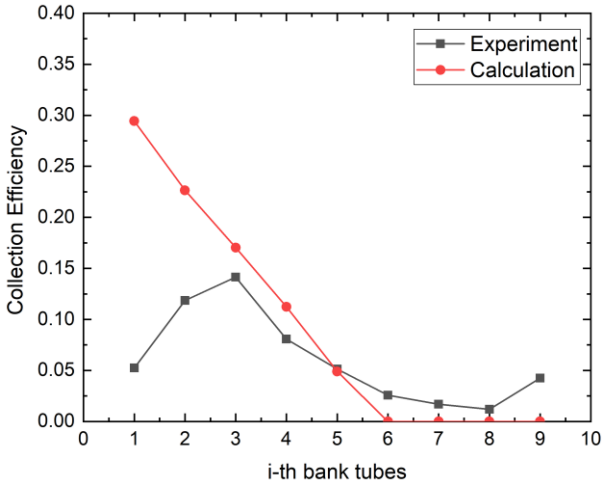

Fig. 4 Measured and calculated aerosol collection efficiencies of i-th bank tubes

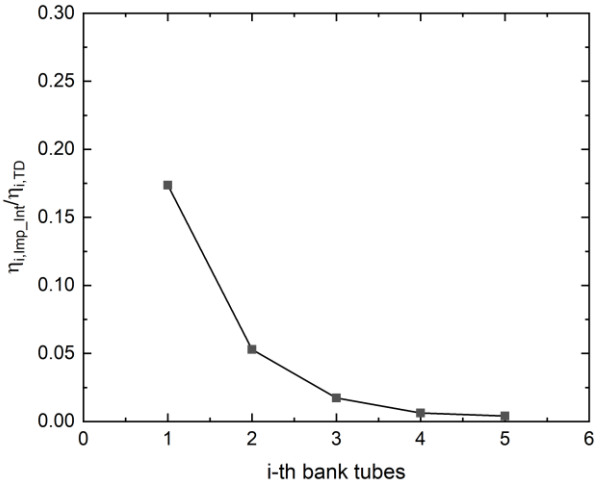

Fig. 5 Collection efficiency of impaction and interception versus turbulent deposition

Figure 5 shows the relative collection efficiency of the impaction and interception divided by that of turbulent deposition. Even for the 1st bank tubes, the turbulent deposition is dominant aerosol collection mechanism on the tube bundle. And on the farther tubes, the contribution of the impaction and interception further decreases. After 6th bank tubes, all the collection efficiency by turbulent deposition, impaction and interception are zero.

The overall collection efficiency by tube bundle was calculated to be 0.38, which is DF of 2.6. The overall DF calculated by the 1-D filter approximation is smaller than those from the experiment. The calculation did not consider the effect of resuspension or rebound of aerosol, as well as the aerosol collection by the z-direction velocity component. Although the 1-D calculation includes a lot of simplification and approximation, still helpful to understand the physics of aerosol removal on the tube bundle.

4. Summary

An aerosol removal by tube bundle in dry SG was tested experimentally, and was estimated using 1-D filter approximation. The bundle made of 270 tubes are installed in the SG vessel, and the aerosol laden hot air was supplied into the vessel. The aerosol concentration was measured by isokinetic sampling at the inlet and outlet of the vessel, and the decontamination factor was estimated from them. The DF for the dry tube bundle was 4.0. After the aerosol test, the tube bundle was disassembled and the aerosol deposited on each tube is collected. The most adjacent tubes from the center showed washed out region near the jet exit, by the kinetic energy of high speed jet. After that, the deposited aerosol mass decreases as the tube becomes farther from the jet exit.

The 1-D analysis of aerosol removal by the tube bundle was conducted with the filter approximation. The collection efficiency of each deposition mechanism was formulated, and the collection efficiency of each tube bank was calculated. The turbulent deposition, impaction, and the interception were included in the calculation.

The calculation shows higher collection efficiency for the close tubes from the center because it does not consider the resuspension or rebound of the aerosol, and shows zero collection behind 6th tube bank. The calculated DF by the calculation was 2.6, lower than the experiment. Despite its simplification, the 1-D calculation provides insight about aerosol removal by dry tube bundle during SGTR.

Acknowledgement

This work was supported by the Korea Institute of Energy Technology Evaluation and Planning (KETEP) grant funded by the Korea government (Ministry of Trade, Industry and Energy) (No.KETEP-20181510102400).

REFERENCES

[1] J. Song, et al., An analysis of the Consequences of a Severe Accident Initiated Steam Generator Tube Rupture, Nuclear Engineering and Design, Vol.348, p14, 2019

[2] C. Zhu et al., Inertial impaction-dominated fibrous filtration with rectangular or cylindrical fibers, Powder Technology, Vol.112, pp.149-162, 2000

[3] L. E. Herranz et al., Major Challenges to Modeling Aerosol Retention near Tube Breach during Steam Generator Tube Rupture Sequences, Nuclear Technology, Vol.158, pp.83-93, 2007